AJNR

Surface-coil MR imaging of orbital neoplasms.

J A Sullivan and S E Harms

AJNR Am J Neuroradiol 1986, 7 (1) 29-34
http://www.ajnr.org/content/7/1/29

Surface-Coil MR Imaging of Orbital Neoplasms

John A. Sullivan[1]
Steven E. Harms[1]

Fifteen patients with orbital neoplasms demonstrated by CT were studied with magnetic resonance (MR) using a 13 cm surface coil and a 0.6 T superconducting magnet. The use of a surface coil allowed for a reduction in slice thickness and a significant improvement in spatial resolution resulting in better demonstration and improved characterization of orbital lesions. All neoplasms (15/15) were demonstrated by MR. The lesions were grouped into four main categories on the basis of signal intensities on T1- and T2-weighted images. CT was superior to MR in displaying densely calcified or bony lesions (two of 15 cases). MR was at least equal or superior to CT in demonstrating the other lesions (13 of 15 cases) and had the added advantage of improved tissue characterization in some cases. With the use of surface coils, MR could become the primary imaging technique for evaluation of orbital neoplasms.

Magnetic resonance (MR) imaging of tissues previously evaluated by other means, specifically computed tomography (CT), has progressed rapidly. MR is a unique imaging method providing information not obtainable by CT. Advantages of MR include lack of potentially harmful ionizing radiation, high soft-tissue contrast resolution without the use of intravenous iodine, its noninvasive nature, direct multiplanar imaging, and absence of beam-hardening artifact that may compromise certain CT examinations. MR has the potential for greater sensitivity and improved specificity compared with CT.

Several investigators have previously applied MR to the orbit [1–10]. Those workers assessing the effectiveness of MR in imaging orbital tumors reached similar conclusions [1–5]. In comparison with CT, MR had no definite diagnostic advantage. Most of the MR examinations, however, were performed at relatively low field strengths (0.15–0.35 T) using conventional head coils as receivers. This instrumentation resulted in a suboptimal signal-to-noise (S/N) ratio for the high-resolution, thin slices needed in orbital studies. Slice thickness ranged from 7 to 12 mm, making partial-volume averaging a problem. The investigators agreed that orbital MR would not become entirely feasible until a means of obtaining increased S/N, with resultant thinner slices and increased spatial resolution, was developed.

With the advent of surface coils, the S/N ratio has increased significantly, making thinner sections and increased spatial resolution possible [10, 11]. With spatial resolution comparable to CT and soft-tissue contrast resolution superior to CT, orbital MR may become very useful in detecting and characterizing lesions. The absence of ionizing radiation and its deleterious effects on the lens is particularly beneficial in orbital examinations [12]. Using a surface coil, we have reassessed the usefulness of MR in evaluation of orbital neoplasms.

Subjects and Methods

Fifteen patients, 2–90 years old, with orbital neoplasms demonstrated by CT were examined with MR. Informed consent was obtained in each case, and the experimental status

Received May 7, 1985; accepted after revision August 27, 1985.

Presented at the annual meeting of the American Roentgen Ray Society, Boston, April 1985.

[1] Department of Medical Imaging, Baylor University Medical Center, 3500 Gaston Ave., Dallas, TX 75246. Address reprint requests to S. E. Harms.

AJNR 7:29–34, January/February 1986
0195–6108/86/0701–0029

of the examination was explained. Surgical pathology was available in 13 of 15 cases.

The studies were performed with a Technicare 1.5 T superconducting magnet operating at a field strength of 0.6 T. The minimum examination consisted of 5 mm axial sections with T1- and T2-weighting, using spin-echo (SE) technique. In some instances, additional planes (i.e., sagittal or coronal) or timing parameters (i.e., spin-density-weighting) were utilized. There was a gap of about 1 mm between adjacent slices.

The routine T1-weighted examination was performed with a repetition time (TR) of 500 msec and an echo time (TE) of 30 msec. The T2-weighted examination had a TR of 2000 msec and a TE of 120 msec. When obtained, spin-density-weighted images had a TR of 1000 msec and a TE of 30 msec. The image display matrix was 256 × 256, and the acquisition matrix was 256 × 256 for T1-weighted examinations and 128 × 256 for T2- and spin-density-weighted exams.

CT was performed in all cases using either a GE CT/T 8800 or a GE CT/T 9800 scanner. The minimum CT examination consisted of contrasted 3–5 mm slices in the axial plane.

The body coil was modified for transmission only. A 13-cm-diam surface coil, designed by Technicare (Solon, OH), was used as a receiver only. A 5 mm foam pad served as a coil spacer, and, in most cases, the coil was centered directly over the orbit of interest. Several examinations were performed with the surface coil positioned over both orbits at once. The patients were instructed to keep their eyes closed during the examination and to refrain from eye movement. Cosmetics were often noted to produce metal artifacts in the images. As a precaution, patients using eye cosmetics were instructed to remove them before the examination.

TABLE 1: **Findings in Patients with Orbital Neoplasms Studied with MR Surface-Coil Imaging**

Standard/Group: Case No. (age, gender), Diagnosis	Relative Signal Intensity		
	T1	T2	N(H)
Retroorbital fat	H	M	H
Vitreous humor	L	H	L
Extraocular muscles	L	L	L
Group 1:			
1 (63, F), Meningioma	L	L	...
2 (28, M), Osteoma	L	L	L
Group 2:			
3 (46, F), Dermoid	H	H	H
4 (44, F), Dermoid	H/L	M/H	H/L
Group 3:			
5 (73, F), Melanoma	M	L	H
6 (25, M), Melanoma	M	L	H
7 (63, M), Melanoma	M	L	H
8 (2, M), Retinoblastoma	M	...	...
9 (2, F), Retinoblastoma	M	L	H
Group 4:			
10 (64, M), Cavernous hemangioma	L	H	...
11 (38, M), Cavernous hemangioma	L	H	...
12 (58, F), Lymphocytic lymphoma	L	H	...
13 (90, F), Lymphocytic lymphoma	M	H	...
14 (73, F), Adenoid cystic carcinoma	M/L	M/H	M
15 (79, M), Basal cell carcinoma	M	H	...

Note.—H = high, M = moderate, and L = low signal intensity.

Results

The clinical data of the 15 patients examined are presented in table 1. Pathologic correlation was available in 13 of 15 cases. Two cases of cavernous hemangioma and one case of optic nerve sheath meningioma were presumed diagnoses on the basis of CT characteristics and the patients' clinical course.

The neoplasms were graded as high, moderate, or low signal intensity on T1-, T2-, and proton density (N[H])-weighted examinations. The signal intensities of retroorbital fat, vitreous humor, and extraocular muscles were used as internal standards (table 1).

MRI demonstrated the orbital lesions in all cases. Of all the tumors imaged, only the two dermoids displayed high signal intensity with T1-weighting. One dermoid was homogeneously hyperintense on all examinations, suggesting a combination of fat and water components. This ovoid, well defined lesion was located in the lacrimal fossa. The CT examination was characteristic, revealing a homogeneous, nonenhancing mass with fat density. The other dermoid (fig. 1) also had high signal intensity on T1-, T2-, and N-weighted studies, but, in this case, a definite fat-fluid level was observed. The dependent layer had signal intensities characteristic of water, while the floating layer had signal intensities characteristic of fat. The lesion was poorly demonstrated by CT.

Two cases of cavernous hemangioma were studied, and the MRI appearances were identical (fig. 2). Both lesions were homogeneous, sharply circumscribed, and intraconal with low signal intensity on T1-weighted images and high signal intensity on T2-weighted images. These lesions were displayed equally well with CT.

A heavily calcified optic nerve sheath meningioma and an orbital osteoma (fig. 3) were the only lesions observed with low signal intensity on both T1- and T2-weighted studies. The meningioma was displayed as a hypointense, poorly defined enlargement of the optic nerve. The size of the lesion was difficult to assess, and the extension through the optic canal was not demonstrated by MR. This neoplasm was unquestionably better demonstrated by CT. The osteoma had a hypointense center, probably representing fibrous tissue, surrounded by a peripheral rim devoid of signal, representing cortical bone. The lesion was very large and displaced the medial rectus muscle as well as the optic nerve laterally.

Although several types of orbital neoplasms had moderate signal intensity on T1-weighted images, only two types (melanoma and retinoblastoma) were hypointense on T2-weighted images. The appearance of melanoma is presumably caused by stable-free radicals within melanin that shorten the T1 and T2 relaxation times [13]. Although the two lesions could not be differentiated from each other by MR signals alone, the clinical settings for these two lesions are usually quite different.

Both cases of retinoblastoma (fig. 4) had moderate signal intensity on T1-weighted studies. A T2-weighted study in one case demonstrated a hypointense, intraocular mass that did not extend beyond the globe. In both cases CT findings were characteristic, revealing enhancing, calcified retinal masses.

The three intraocular melanomas (fig. 5) had identical signal characteristics, that is, moderate, low, and high intensity on T1-, T2-, and N-weighted examinations, respectively. Two

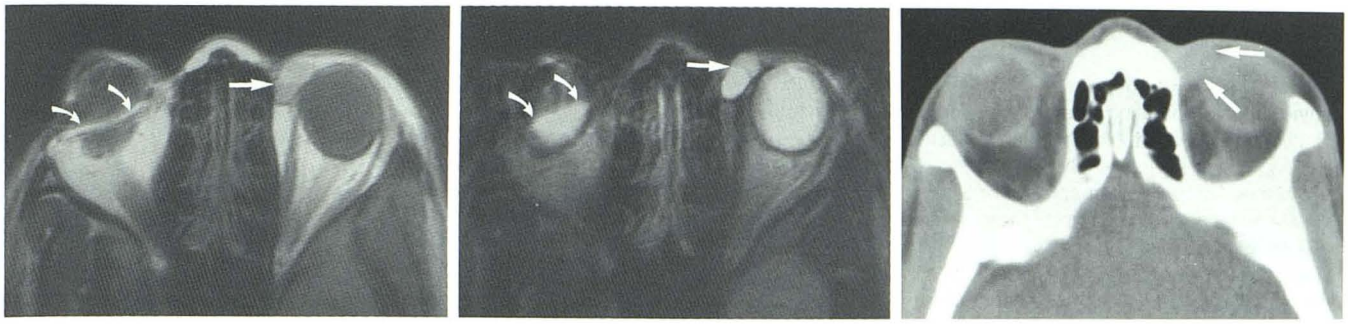

Fig. 1.—Dermoid. SE 1000/30 (**A**) and SE 2000/120 (**B**) images and unenhanced CT scan (**C**). Fat-fluid level within dermoid (*straight arrows*) was well demonstrated by MR. Eye cosmetics degrade image (*curved arrows*). Lesion was poorly demonstrated by CT.

Fig. 2.—Cavernous hemangioma. SE 500/30 (**A**) and SE 2000/120 (**B**) images. Lesion seen well on both images because of contrast with retroorbital fat.

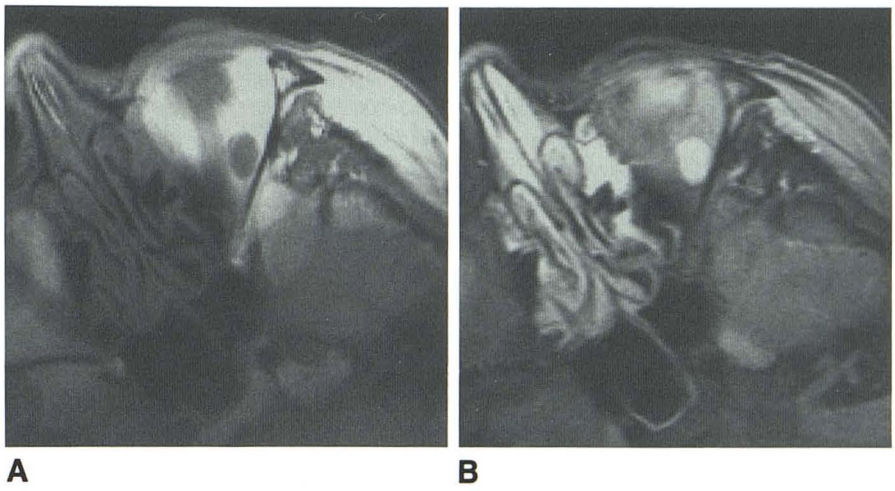

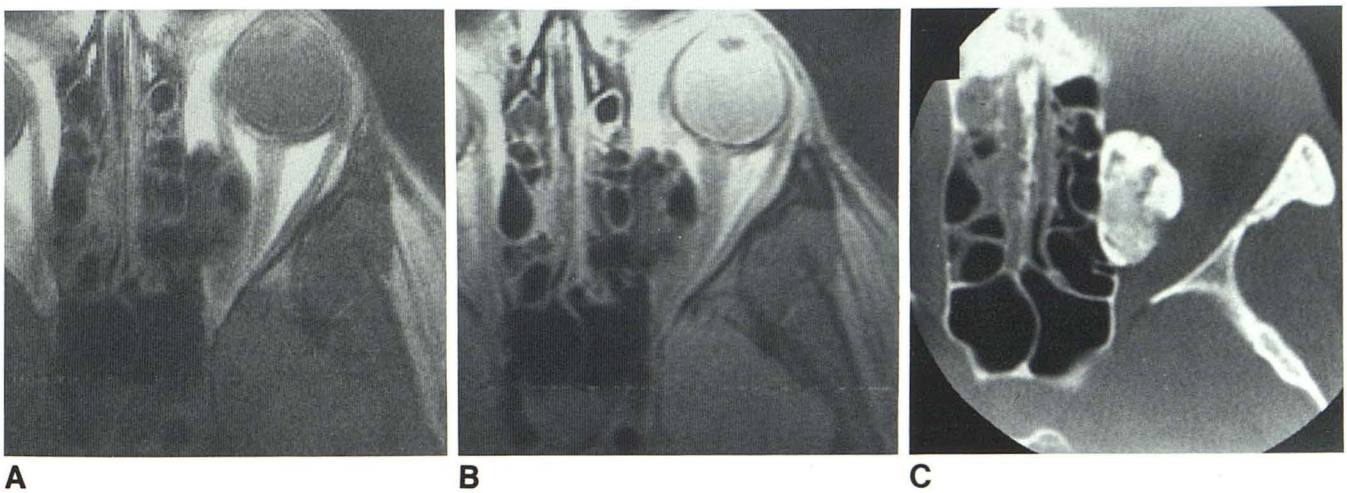

Fig. 3.—Osteoma. SE 500/30 (**A**) and SE 1000/30 (**B**) images and contrast-enhanced CT scan (**C**). Bony lesion displaces medial rectus muscle and optic nerve in patient with Gardner syndrome. Lesion was much better demonstrated by CT.

lesions were associated with a subretinal fluid collection secondary to retinal detachment which had high signal intensity on both T1- and T2-weighted examinations. On T2-weighted studies, however, the hypointense tumor mass could be delineated from the surrounding fluid. MR was better than CT in demonstration and characterization of intraocular melanomas.

On T1-weighted examinations, low or moderate signal in-

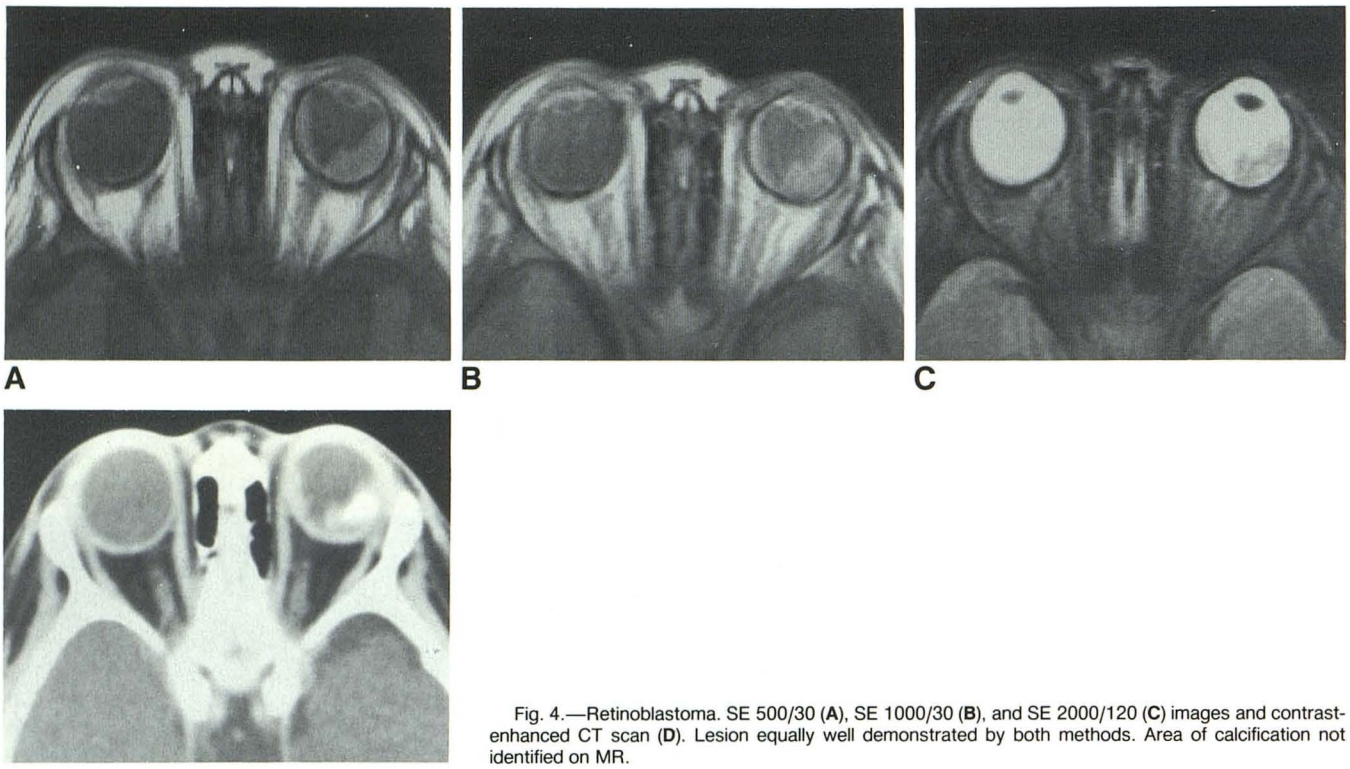

Fig. 4.—Retinoblastoma. SE 500/30 (**A**), SE 1000/30 (**B**), and SE 2000/120 (**C**) images and contrast-enhanced CT scan (**D**). Lesion equally well demonstrated by both methods. Area of calcification not identified on MR.

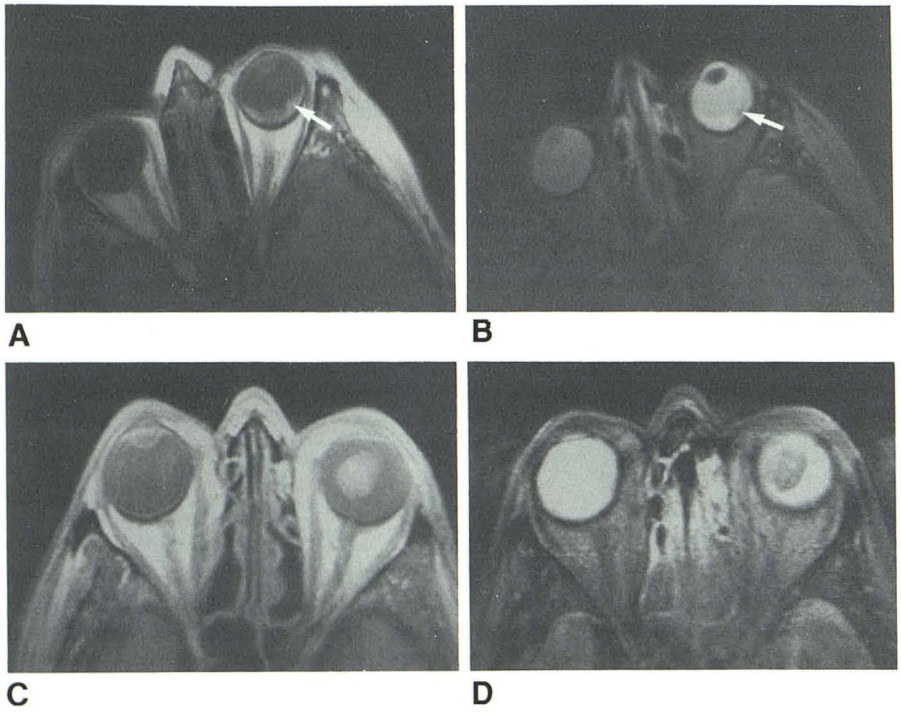

Fig. 5.—Melanoma. SE 500/30 (**A**) and SE 2000/120 (**B**) images. Tumor nidus (*arrows*) can be separated easily from serous subretinal fluid collection. In a different case, SE 1000/30 (**C**) and SE 2000/120 (**D**) images show melanoma without subretinal fluid and demonstrate characteristic low signal intensity on T2-weighted study.

tensity was observed in two cases of orbital lymphocytic lymphoma (fig. 6). Both of these lesions were hyperintense on T2-weighted studies, however. In one case, infiltration of the medial rectus muscle and retroorbital fat was better demonstrated with MR than with CT because of the long T2 of the tumor. The other case of lymphoma involved the lacrimal gland and was displayed equally well by CT.

Both adenoid cystic carcinoma (fig. 7) and basal cell carcinoma were of moderate signal intensity on T1-weighted studies. In contrast to melanoma, however, both lesions became hyperintense with increased T2-weighting. The adenoid cystic carcinoma arising in the lacrimal gland had a necrotic center

Fig. 6.—Lymphocytic lymphoma. SE 500/30 (**A**) and 2000/120 (**B**) images. Extent of neoplasm is well demonstrated because of long T2 of lesion.

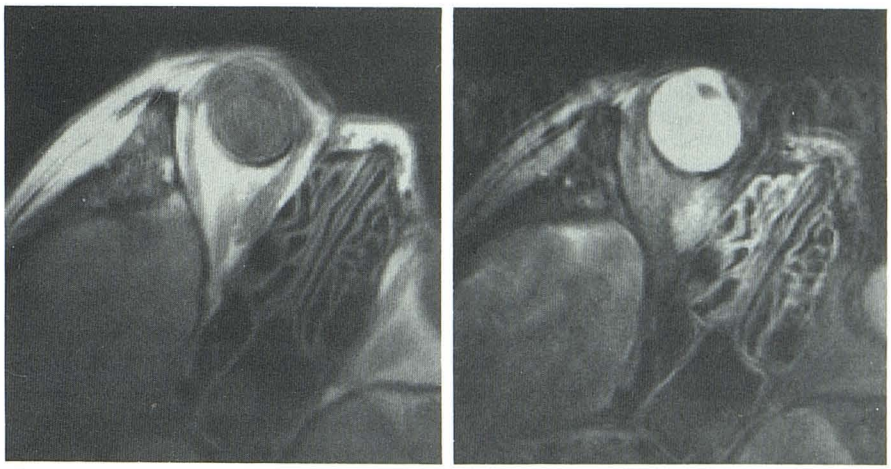

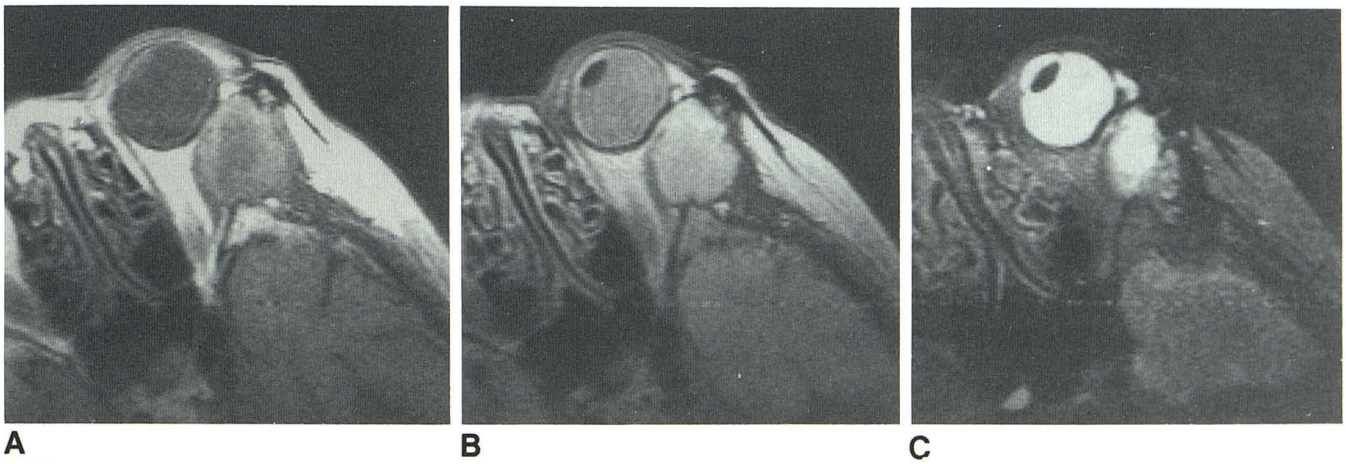

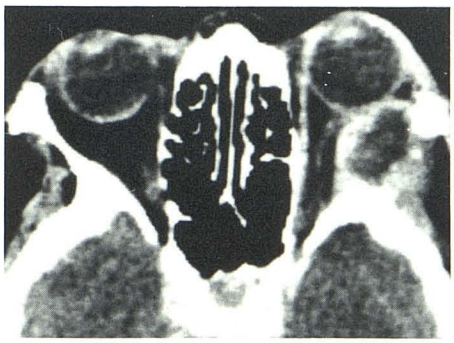

Fig. 7.—Adenoid cystic carcinoma. SE 500/30 (**A**), SE 1000/30 (**B**), and SE 2000/120 (**C**) images and contrast-enhanced CT scan (**D**). Anatomy is best demonstrated on spin-density-weighted image (**B**). T1- (**A**) and T2- (**C**) weighted images reveal area of central necrosis. Erosion through lateral orbital wall is better demonstrated on CT.

with signal characteristics similar to vitreous humor. Both lesions were demonstrated equally well by CT.

Discussion

Examination of the orbit by high-resolution CT has been quite effective, replacing earlier, more invasive diagnostic studies [14, 15]. Because of the markedly different T1 and T2 relaxation values of orbital tissues, however, MR offers superior contrast resolution relative to CT. In addition, the lack of ionizing radiation and the fact that intravenous contrast agents are not needed are distinct advantages. In comparison with CT, the main disadvantage of MR has been inadequate spatial resolution. With the advent of surface coils, this problem has been rectified. Because the S/N ratio is increased by using surface coils,the slice thickness may be reduced and the spatial resolution of superficial tissues is at least as good as, if not better than, high-resolution CT. The signal characteristics of the various neoplasms imaged in this study are similar to those obtained by two different groups of investigators [4, 5]. Although further research is needed, the potential for pathologic specificity for some orbital lesions appears promising.

On the basis of similarities and differences in signal char-

acteristics, the nine types of orbital neoplasms studied were grouped into four categories. The first of these includes lesions with low signal intensity with T1- and T2-weighting (i.e., osteoma and optic nerve sheath meningioma). These lesions were densely calcified, and the low mobile proton density accounted for their appearance. Although these neoplasms were demonstrated by MR, they were much better displayed by CT. In cases where the diagnosis is not evident before the examination, MR may adequately detect these lesions and provide some characterization. However, CT should remain the preferred method of evaluation for orbital lesions that are heavily calcified or involve bone.

The second group of lesions are those that had high signal intensity (i.e., equal to retroorbital fat) on T1-weighted examinations. The only lesions imaged with this appearance were dermoids. Conceivably, a hemorrhagic lesion could also appear in this manner.

The third group of neoplasms, which were malignant, had moderate signal intensity on T1-weighted studies and low signal intensity on T2-weighted studies. Only two types of lesions (i.e., melanoma and retinoblastoma) were included in this category. The serous subretinal fluid collection in two cases of melanoma appeared hyperintense on both T1- and T2-weighted examinations, but the tumor nidus could be differentiated easily on the T2-weighted images. Pathologically, the subretinal fluid was not hemorrhagic in nature, and the relatively short T1 was probably from the protein content of the serous fluid. Most ocular melanomas described in the recent literature have been hyperintense on T2-weighted studies. Our results differed, but our examinations were significantly more T2-weighted with a TE of 120 msec versus 56 msec [4] and 90 msec [5] in the other studies. In addition, our slice thickness was 5 mm compared with 7 mm and 8 mm, respectively, in the other studies. The techniques used in previous studies had reduced T2 contrast, and the thicker slices resulted in greater volume averaging. Also, some of the variability in relaxation values is probably related to melanin concentration. MR may be useful in differentiating primary melanoma from metastatic disease.

The calcifications present in both cases of retinoblastoma were not detected by MR. This was not essential to diagnosis, however. In our experience, calcification must be very dense (i.e., Hounsfield numbers approaching those of cortical bone) to be detected by MR, and it is usually better displayed on examinations with relatively long TE values.

The fourth group of orbital neoplasms included those that became more intense with increased T2-weighting (i.e., cavernous hemangioma, lymphocytic lymphoma, basal cell carcinoma, and adenoid cystic carcinoma). These lesions were exceptionally well demonstrated because of the contrast with retroorbital fat. In this category, signal characteristics could not be used to distinguish benign from malignant lesions. The location and margins of the tumor were most useful in making this distinction.

To obtain consistent image quality the radiofrequency (RF) pulses were tuned to 90° and 180° before each study. This added about 10 min to the examination time. The image quality was also degraded by eye movement, particularly when long TEs were used. In our series, movement was not severe enough to affect the diagnostic quality of any of the studies. Also, eye cosmetics were noted to significantly degrade the image quality, presumably from the metal content (fig. 1).

In conclusion, with the proper use of surface coils, we believe that MR is superior to CT for imaging most orbital neoplasms. Not only are the lesions well demonstrated, but in some cases pathologic specificity is obtainable. This is also likely to improve in the future as more lesions are better characterized. MR was definitely superior to CT for imaging ocular lesions, and pathology as well as normal anatomy were well displayed. With the present technology, MR could be used as the primary diagnostic imaging procedure for orbital lesions.

Further technical improvements should make orbital MR even better. Elimination of slice gaps and decreasing the slice thickness are needed to optimize orbital MR. Potentially, these goals can be accomplished in two different manners. Using a square RF pulse with 2D imaging techniques allows for thin (i.e., <2 mm), nearly contiguous slices. Similar results can be obtained using 3D imaging techniques by selectively exciting a volume or "slab" of tissue and further subdividing this into thin, contiguous slices.

REFERENCES

1. Li KC, Poon PY, Hinton P, et al. MR imaging of orbital tumors with CT and ultrasound correlations. *J Comput Assist Tomogr* **1984**;6:1039–1047
2. Hawkes RC, Holland GN, Moore WS, Rizk S, Worthington BS, Kean DM. NMR imaging in the evaluation of orbital tumors. *AJNR* **1983**;4:254–256
3. Han JS, Benson JE, Bonstelle CT, Alfidi RJ, Kaufman B, Levine M. Magnetic resonance imaging of the orbit: a preliminary experience. *Radiology* **1984**;150:755–759
4. Sobel DF, Kelly W, Kjos BO, Char D, Brant-Zawadzki M, Norman D. MR imaging of orbital and ocular disease. *AJNR* **1985**;6:259–264
5. Edward JH, Hyman RA, Vacirca SJ, et al. 0.6 T magnetic resonance imaging of the orbit. *AJNR* **1985**;6:253–258
6. Sobel DF, Mills C, Char D, et al. NMR of the normal and pathologic eye and orbit. *AJNR* **1984**;5:345–350
7. Moseley I, Brant-Zawadzki M, Mills C. Nuclear magnetic resonance imaging of the orbit. *Br J Ophthalmol* **1983**;67:333–342
8. Daniels DL, Herfkins R, Gager WE, et al. Magnetic resonance imaging of the optic nerves and chiasm. *Radiology* **1984**;152:79–83
9. Sassani JW, Osbakken MD. Anatomic features of the eye disclosed with nuclear magnetic resonance imaging. *Arch Ophthalmol* **1984**;102:541–546
10. Schenck JF, Hart HR, Foster TH, et al. Improved MR imaging of the orbit at 1.5 T with surface coils. *AJNR* **1985**;6:193–196
11. Schenck JF, Foster TH, Henkes JL, et al. High-field surface-coil MR imaging of localized anatomy. *AJNR* **1985**;6:181–186
12. Lund E, Malaburt M. Irradiation dose to the lens of the eye during CT of the head. *Neuroradiology* **1982**;22:181–184
13. Damadian R, Zaner K, Hor D. Brain tumors by NMR. *Physiol Chem Phys* **1973**;5:381–402
14. Weinstein MA, Modic MT, Risius B, Duchesneau PM, Berlin AJ. Visualization of the arteries, veins, and nerves of the orbit by sector computed tomography. *Radiology* **1981**;138:83–87
15. Hammerschlag SB, Hesselink JR, Weber AL. *Computed tomography of the eye and orbit.* East Norwalk, CT: Appleton-Century-Crofts, **1983**